A Green Synthesis of Mn_3O_4/graphene Nanocomposite as Anode Material for Lithium-Ion Batteries

Ning-Jing Song[1,*], Canliang Ma[2,*]

[1] College of Chemistry and Chemical Engineering, Jinzhong University, Jinzhong, 030619, PR China
[2] Key Laboratory of Materials for Energy Conversion and Storage of Shanxi
Province, Institute of Molecular Science, Shanxi University, Taiyuan 030006, PR China
*E-mail: macanliang@sxu.edu.cn

A green and gentle synthesis method of Mn_3O_4/graphene nanocomposite is supplied to achieve a high property anode material for Li-ion batteries. The synthesis process of Mn_3O_4/graphene nanocomposites consists of two parts: one is the formation of Mn_3O_4 nanoparticles by hydrothermal reaction; the other is the reduction of graphene oxide to graphene by Vitamin C in hot bath, companied with the combination of graphene and Mn_3O_4. During the preparation process, all raw materials and by-products are non-toxic, meanwhile, the methods are green, gentle and energy saving. The resulting materials are characterized by XRD, SEM and TG. The composite materials deliver a stable reversible capacity of 500 mA h g^{-1} at a current density of 100 mA g^{-1} even after 100 cycles. The reversible capacity of the samples coated by crumpled graphene is higher than pure Mn_3O_4 nanoparticles. This research supplies a new effective strategy to fabricate metal oxide/graphene nanocomposites with high electrochemical performances anode materials through a real environmental friendly method.

1. INTRODUCTION

In the last two decades, Li-ion batteries (LIBs), a kind of promising energy systems, have attracted much attention, which may be attributed to their long cycle life, high energy density, and environmental benignity[1]. As commercial anode material, graphite materials could only deliver a specific capacity of 372 mA h g^{-1}, which is difficult to meet the increasing demand for the higher energy density and power density[2,3]. Thus, some new high-capacity materials are studied for

improving the energy and power densities of LIBs, such as silicon, tin and metal oxides with various nanostructures and morphology features[4-6]. Among them, manganese oxides (Mn_3O_4), with the high theoretical lithium-storage capacities (936 mA h g^{-1}), low price and natural abundance, has been widely studied as an anode electrode for LIBs[1][7]. Nowadays, there are many methods for the synthesis of Mn_3O_4, such as organic solvent-assisted thermal decomposition [8], polymeric-precursor [9], microwave-assisted [10], surfactant-mediated [11], and solvothermal [12] routes. Among these methods, some organic solvent may be used as the raw material, or some toxic by-products may be produced. However, most of the organic solvents and toxic by-products would cause pollution and increase the cost of LIBs, which adverse to the promotion of novel anode materials. Thus, it is necessary to develop a green method to prepare high-performance manganese oxides as anode materials.

In the other side, the shortcomings of Mn_3O_4, including high electrical resistance, poor electrochemical reversibility and low electrical conductivity, make it difficult to be alone used for anode materials of LIBs[13]. An effective solution is to prepare a composition of Mn_3O_4 and carbon materials. Graphene, as a kind of new carbon material, which has excellent flexibility, large specific surface area and high electrical conductivity, is suitable for using as the support of transition metal oxide nanoparticles for anode materials[14]. Now, Mn_3O_4/graphene nano-composites synthesized through many different methods are verified to be high-capacity and excellent cycle stability materials. Crumpled graphene has been further proved to be useful for improving the power capability and cycle stability of battery [15-17]. Luo et al has prepared crumpled graphene by a rapid, one-step capillary-driven assembly route in aerosol droplets[16]. However, the method needs to consume vast amounts of extra energy, which is opposite to environmentally friendly products.

According to the above analysis about the preparation of Mn_3O_4 nanoparticles and Mn_3O_4/graphene nano-composites, many works need to be done to synthesize high-performance anode materials for LIBs through a green method. Herein, in the present work, deionized water, absolute ethyl alcohol and $KMnO_4$ are selected as the raw materials, simple hydrothermal method is used. Mn_3O_4 nanoparicles are wrapped by crumpled graphene which is reduced by Vitamin C (VC) at 95 ^{o}C. As a result, a 3- dimension (3D) Mn_3O_4/graphene nano-composites are synthesized. The synthesis process of Mn_3O_4/graphene nanocomposites consists of two parts: one is the formation of Mn_3O_4 nanoparticles, the other is the reduction of graphene oxide (GO) to graphene, combined with the composite of graphene and Mn_3O_4. During the whole process, any raw materials and by-products are non-toxic. The method is simple, green and energy saving. The structure of 3D Mn_3O_4/graphene nano-composites is benefit to enhance energy and power densities of LIBs.

2. EXPERIMENT DETAILS

2.1 Preparation of Mn_3O_4 nanoparticle

0.5 g of $KMnO_4$ was dissolved into a 40 mL mixture solution that contained 20 mL deionized water and 20 mL ethanol to obtain a brownish precipitate. Then well-dispersed brownish suspension

solution was transferred into a Teflon-lined stainless steel autoclave to maintain at 180 $^{\circ}$C for 12 h. Finally, the products were filtered and cleaned with deionized water for several times, followed by drying at room temperature. The material was marked as Mn_3O_4.

2.2 Preparation of Mn_3O_4/graphene composite

40 mg of graphite oxide and 50 mg of Mn_3O_4 were dispersed in 40 mL of deionized water using ultrasonication for 2 h. Then 20 mg of ascorbic acid was well dispersed in 40 mL of GO solution. The homogeneous suspension was stirred at 95 $^{\circ}$C for 20 min, during which GO sheets was reduced to crumpled graphene. The final product was filtered by vacuum filtration method and dried at room temperature. The material was marked as Mn_3O_4/G.

2.3 Material characterization

The as-obtained samples were characterized by using a scanning electron microscope (SEM, JSM-7001F, 3.0 kV), an X-ray diffractometer (XRD, Cu Ka radiation, D8 Advance, BRUKER/ AXS, Germany), thermogravimetric analysis (TG, TA Q600 instrument).

2.4 Electrochemical measurements

The electrochemical properties are measured using coin-type (CR2016) half cells. 80 wt.% samples ,10 wt.% acetylene black and 10 wt.% PVDF were mixed with NMP to produce slurry. Then the slurry is uniformly loaded on a Cu foil with a doctor blade to prepare a film-type electrode. The sample is dried for 12 h under a vacuum at 120 $^{\circ}$C, followed by cut into circular electrodes. The cells are assembled in an Ar-filled glove box with lithium foil as both reference and counter electrode, and a solution of 1.0 M $LiPF_6$ dissolved in 1 : 1 (v/v) EC/DEC as the electrolyte. All electrochemical measurements are carried out on a battery testing system (LAND CT 2001A) in the potential range from 0.01 V to 3 V (vs. Li^+/Li). Electrochemical impedance spectroscopy (EIS) are measured in the frequency range from 100 kHz to 0.01 Hz with alternating-current (AC) signal amplitude of 0.5 mV.

3. RESULTS AND DISCUSSION

The phase components of the synthesized samples are confirmed by XRD (Fig. 1). It is found that the typical diffraction peaks of Mn_3O_4 at 18°, 28.9°, 31.0°, 32.3°, 36.1°, 37.9°, 44.4°, 50.7°, 53.8°, 56.0°, 58.5°, 59.8°, 64.6° (JCPDS No. 24-0734), which indicates that Mn_3O_4 has been synthesized by hydrothermal method and has better crystal. For Mn_3O_4/graphene composite, the peaks of Mn_3O_4 don't change, which indicated that the crystal forms of Mn_3O_4 nanoparticles has not been changed during

chemical reduction process, meanwhile, the peak appeared at 26.1° (JCPDS No. 65-6212) shows that GO sheets (2θ = 12.5°)[18] have been effectively exfoliated and transformed into graphene.
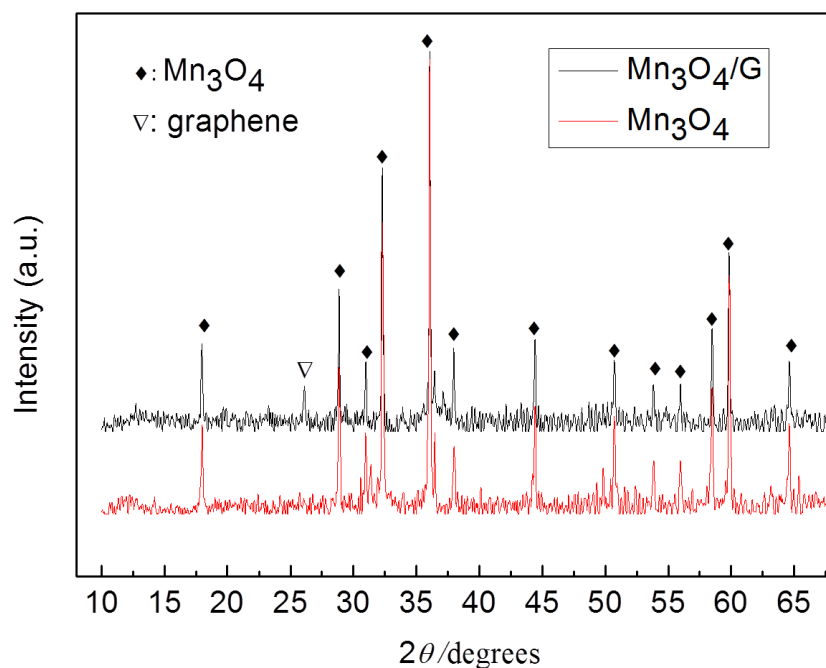

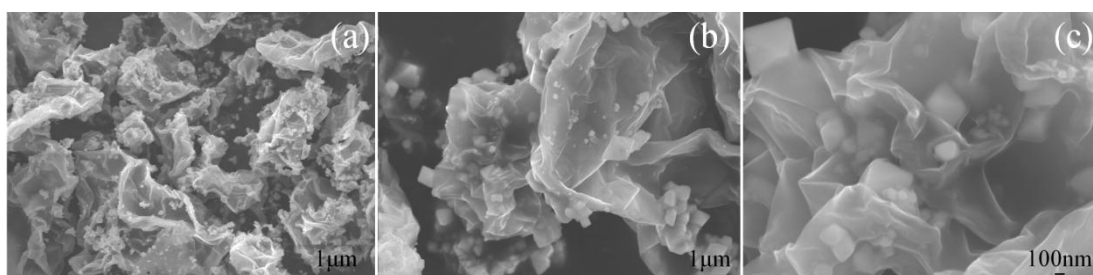**Figure 1.** XRD spectra of Mn_3O_4 and Mn_3O_4/graphene composite

Figure 2. SEM image of Mn_3O_4/graphene composite, (a) low-, (b) middle-, (c) high- resolution

As shown in Fig.2a, some 3D composites are observed. During the chemical reduction process, GO sheets become crumpled balls owing to the oxygen-functionalities missing and stirring, meanwhile, Mn_3O_4 nanoparticles are closely attached and coated by crumpled graphene balls. The crumpled graphene balls are remarkably stable, which may be attributed to $\pi-\pi$ stacked fold during the reduction process. The crumpled morphology of graphene balls prevents the aggregation of graphene sheets and Mn_3O_4 nanoparticles. The obtained Mn_3O_4 nanoparticles exhibit octahedron-like morphology, which shows that high-quality Mn_3O_4 has been prepared by simple and green hydrothermal method (Fig.2b). Mn_3O_4 nanoparticles were wrapped by the crumpled graphene sheets (Fig.2c). The structure makes the contact between crumpled graphene sheets and Mn_3O_4 nanoparticles easier.
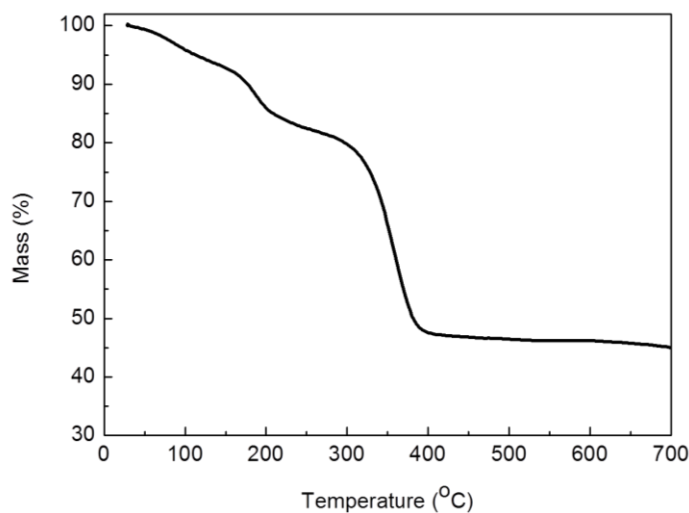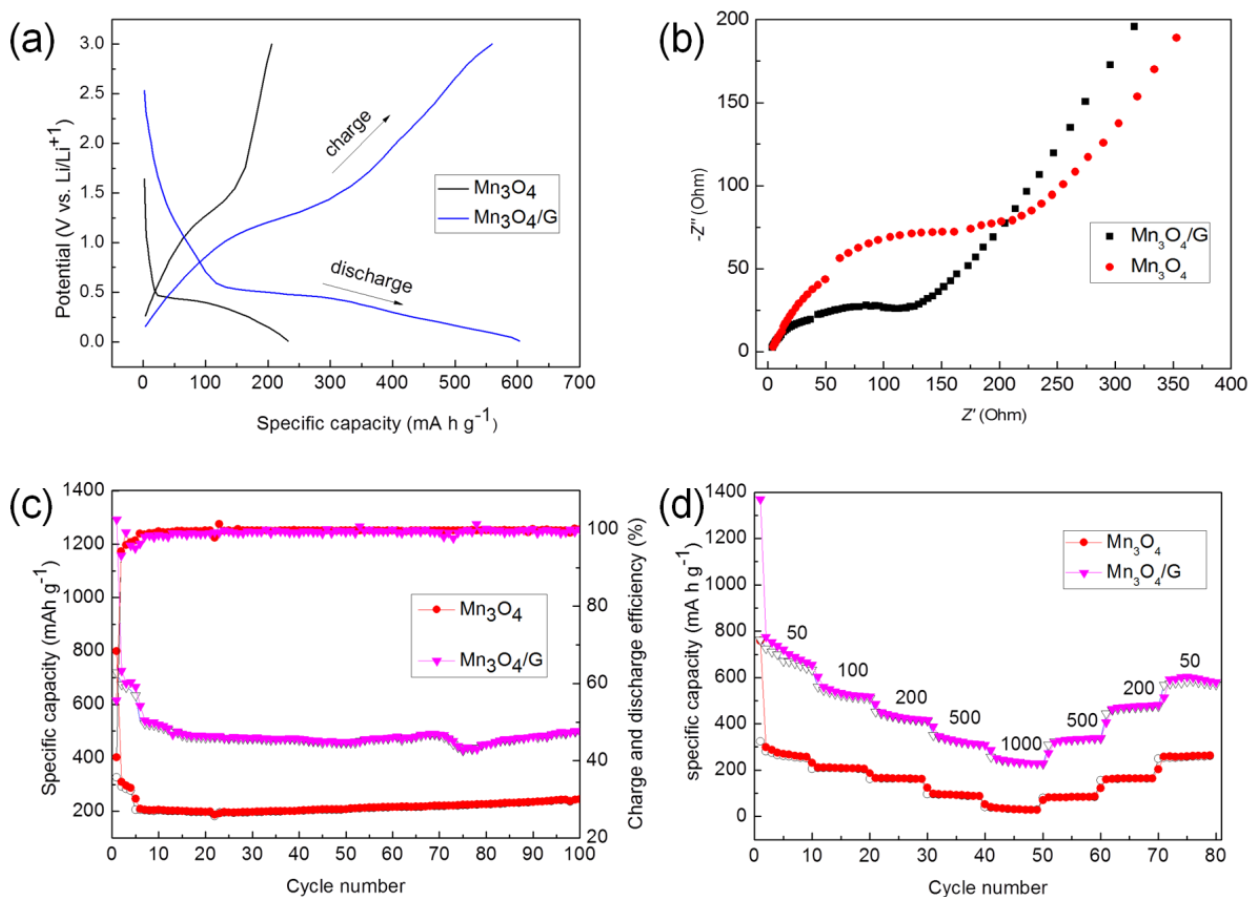
Figure 3. TGA profile of Mn_3O_4/graphene composite

Figure 4. a) charge-discharge profiles of Mn_3O_4 and Mn_3O_4/graphene electrodes at a current density of 100 mA g^{-1}; b) the Nyquist plots of Mn_3O_4 and Mn_3O_4/graphene electrodes; c) The comparison of the discharge–charge capacity between the Mn_3O_4 and Mn_3O_4/graphene electrodes at a current density of 100 mA g^{-1} for 100 cycles; d) the rate capability of the Mn_3O_4 and Mn_3O_4/graphene electrodes

Table 1. the comparison of different anode materials

Anode material	Synthesis method	Raw material	Current density (mA g^{-1})	capacity (mA h g^{-1})	reference
Mn$_3$O$_4$/ graphene composites	One step hydrothermal synthesis	MnCl$_2$·4H$_2$O, PVP, GO, NH$_3$, NaBH$_4$,	60	500	[1] One step hydrothermal synthesis of Mn3O4/ graphene composites with great electrochemical properties for lithium-ion batteries
Graphene/Mn$_3$O$_4$ Nanocomposite Membrane	Two step hydrothermal synthesis	MnSO$_4$, KClO$_3$, CH$_3$COOK, CH$_3$COOH, GO	100	702	[2] Highly Flexible Graphene/Mn3O4 Nanocomposite Membrane as Advanced Anodes for Li-Ion Batteries
Mn$_3$O$_4$ nanorod/reduced graphene oxide hybrid paper	vacuum filtration and thermal treatment	KMnO$_4$, polyethylene glycol 400, GO	100	573	[3] Porous Mn3O4 nanorod/reduced graphene oxide hybrid paper as a flexible and binder-free anode material for lithium ion battery
Mn$_3$O$_4$/graphene Nanocomposite	hydrothermal synthesis and low temperature reduction	KMnO$_4$, ascorbic acid, GO	100	500	This work

The content of Mn$_3$O$_4$ in the composite is measured by TGA. The sample is oxidized in air from room temperature to 700 $^{\circ}$C with 10 $^{\circ}$C/min. As shown in Fig. 3, Weight loss at ~100 $^{\circ}$C is attributed to the volatilization of water. The main weight loss occurs from 150 to 380 $^{\circ}$C, which is due to oxygen-containing functional groups decomposing into CO, CO$_2$, and water vapor[19]. The mass loss do not change when the temperature rises from 400 to 700 $^{\circ}$C, demonstrating the residual mass maybe Mn$_3$O$_4$ nanoparticles. Thus, the mass content of Mn$_3$O$_4$ and graphene are estimated to be 46.22% and 53.78%, respectively. On the basis of these data and the theoretical specific capacity of

graphene and Mn_3O_4, the theoretical specific capacity of the sample could be figured out with the formula.

$$Sum = 744 \text{ mA h g}^{-1} * 53.78\% + 936 \text{ mA h g}^{-1} * 46.22\% = 832.74 \text{ mA h g}^{-1}$$

Typical discharge/charge curves of Mn_3O_4 and Mn_3O_4/graphene electrodes at a current density of 100 mA g^{-1} over a voltage range of 0.001-3.0 V vs. Li/Li$^+$ was shown in Fig.4a. Mn_3O_4/graphene shows the higher discharge capacity (600 mA h g^{-1}) than Mn_3O_4 (230 mA h g^{-1}). The discharge capacity in the range of 1.4-0.5 V was mainly due to reduction from Mn(III) to Mn(II), and the 0.5-0.1 V range reflected the reduction from Mn(II) to Mn(0)[20]. In the relative charge process, the charge capacity below the voltage 1.3 V is mainly due to reduction from Mn(III) to Mn(II) and then to Mn(0) [21]. More charge capacity of Mn_3O_4/graphene nanocomposite than Mn_3O_4 above the voltage 1.3 V comes from the delithiation of graphene[21]. Obviously, Mn_3O_4/graphene nanocomposite exhibits longer platform and larger reversible capacity, which should be contributed to the good support of crumpled graphene.

The Nyquist plots of Mn_3O_4 and Mn_3O_4/graphene electrodes consist of two parts: a semicircle in the high frequency and a slope line in the low frequency. The semicircle may be resulted from two parts: 1)Li$^+$ migration resistance through the SEI film, 2)the charge-transfer resistance at the electrode surface [22,23]. Meanwhile, the slope line could be attributed to the diffusion of lithium ions into electrode materials [22,23]. As shown in Fig.4b, compared with Mn_3O_4 electrodes, Mn_3O_4/graphene electrodes exhibit larger slope in the low frequency region, indicating faster Li$^+$ diffusion rates for Mn_3O_4/graphene electrodes[24]. The diameter of the high-frequency semicircle of Mn_3O_4/graphene electrodes is much smaller than that of Mn_3O_4 electrodes, revealing lower migration and charge-transfer resistances, which may be attributed to the highly electric conduction performance of graphene sheets. Thus, graphene sheets, a highly conductive matrix, may have a significant contribution to the higher discharge-charge capacity and better rate capability of Mn_3O_4/graphene electrodes.

Fig. 4c displays the comparison of the discharge-charge capacity between the Mn_3O_4 and Mn_3O_4/graphene electrodes at the current density of 100 mA g^{-1} for 100 cycles. In the initial cycle, the discharge and charge capacity of the Mn_3O_4/graphene electrode are ca. 1292.7 mA h g^{-1} and ca. 719.5 mA h g^{-1}, respectively, the initial coulombic efficiency is 55.6%. The large irreversible capacity loss is due to the inevitable solid electrolyte interface (SEI) film formation on the electrode surface and some possible side reactions between Li$^+$ and the residual functional groups in the graphene structure[25]. With the ongoing cycling, the capacity of the samples is stable because of the gradually improved stability of the material structure. Compared with pure Mn_3O_4 (244 mA h g^{-1}), Mn_3O_4/graphene delivers a high specific capacity 500 mA h g^{-1} after 100 cycles, indicating that graphene sheets contribute significantly to the specific capacity retention.

The synthesis method, raw material, current and capacity of different anode materials were shown in Table 1. From this, we can find that the capacity of the anode materials prepared by others are just a little higher than the anode material in our work. However, the raw materials used in our work is more green and cleaner, the synthesis method is more simple and energy-saving.

As shown in Fig.4d, the rate capability of Mn_3O_4 and Mn_3O_4/graphene electrodes are measured at current densities of 50, 100, 200, 500, 1000 mA g^{-1}, respectively. The reversible capacities of Mn_3O_4 electrode are ca.261.9, 207.7, 162.9, 91.9, 31.4 mA h g^{-1}, respectively. Meanwhile, those of

Mn_3O_4/graphene electrode are ca.670.8, 524.6, 426.8, 324.8, 236.1 mA h g^{-1}, respectively. When the current densities are reset to 500, 200, 50 mAg^{-1}, the reversible capacities of Mn_3O_4 and Mn_3O_4/graphene electrodes return to ca.83.8, 164.1, 257.1 and 330.9, 469.7, 604.0 mA h g^{-1}, respectively. The data demonstrate that both Mn_3O_4 and Mn_3O_4/graphene electrodes have stable structure and rate capability. The capacities of Mn_3O_4/graphene are always higher than that of Mn_3O_4 electrodes, which may be attributed to the support of crumpled graphene sheets[16]. Crumpled graphene sheets supply not only great current network but also enough spaces for the huge volume expansion of Mn_3O_4. Thus, Mn_3O_4/graphene nanocoposites could retain stable structures and hold long life and high reversible capacity.

4. CONCLUSION

3D Mn_3O_4/graphene nano-composition has been synthesized by hydrothermal method and chemical reduction. During the process, any raw materials and by-products are non-toxic. The used method is simple, green and energy saving. During the chemical reduction process, GO sheets become crumpled graphene balls and Mn_3O_4 nanoparticles were wrapped by graphene sheets. The structure of Mn_3O_4/graphene nano-composition is stable and benefit to improve the electrochemical performance of LIBs. The composite materials deliver a stable reversible capacity of 500 mA h g^{-1} at a current density of 100 mA g^{-1} even after 100 cycles. The reversible capacity of the samples coated by graphene is much better than pure Mn_3O_4 nanoparticles. Thus, it is a green and effective preparation strategy of Mn_3O_4/graphene nanocomposites as anode material for LIBs.

References

1. M.S. Whittingham, *Chem. Rev.* , 104 (2004) 4271.
2. H. Li, Y. Wei, Y. Zhang, C. Zhang, G. Wang, Y. Zhao, F. Yin and Z. Bakenov, *Ceram. Int.,* 42 (2016) 12371.
3. W. Zhang, Y. Zeng, N. Xiao, H.H. Hng and Q. Yan, *J. Mater. Chem.*, 22(2012) 8455.
4. S.K. Park, S.H. Yu, S. Woo, J. Ha, J. Shin, Y.E. Sung and Y. Piao, *CrysteEngcomm.*, 14 (2012) 8323.
5. W. Shi and B. Lu, *Electrochim. Acta*, 133(2014) 247.
6. B. Liang, Y. Liu and Y. Xu, *J. Power Sources*, 267 (2014) 469.
7. I. Nam, N.D. Kim, G.P. Kim, J. Park and J. Yi, *J. Power Sources*, 244 (2013) 56.
8. Y.P. Du, Y.W. Zhang, L.D. Sun and C.H. Yan, *J. Phys. Chem.* C, 113 (2009) 6521.
9. W.S. Seo, H.H. Jo, K. Lee, B. Kim, S.J. Oh and J.T. Park, *Angew. Chem.Int. Ed.*, 43(2004) 1115.
10. L.X. Yang, Y.J. Zhu, H. Tong, W.W. Wang and G.F. Cheng, *J. Solid State Chem.*, 179 (2006) 1225.
11. P. Li, C. Nan, Z. Wei, J. Lu, Q. Peng and Y. Li, *Chem. Mater.*, 22(2010) 4232.
12. K. Ahmed, Q. Zeng, K. Wu and K. Huang, *J. Solid State Chem.*, 183(2010) 744.
13. C. Wang, L. Yin, D. Xiang and Y. Qi, *ACS Appl. Mater. Interfaces* 4 (2012) 1636.
14. L. Torres, S. Roche and J.C. Charlier, *Introduction to Graphene-Based Nanomaterials: From Electronic Structure to Quantum Transport,* (2014) Cambridge University Press.

15. Y.S. Yun, Y.U. Park, S.J. Chang, B.H. Kim, J. Choi, J. Wang, D. Zhang, P.V. Braun, H.J. Jin and K. Kang, *Carbon*, 99(2016) 658.
16. J. Luo, X. Zhao, J. Wu, H.D. Jang, H.H. Kung and J. Huang, *J. Phys. Chem. Lett*., 3 (2012) 1824.
17. C. Ma, J. Shi, Y. Zhao, N.J. Song and Y. Wang, *Chem. Eng. J.* ,326 (2017) 507.
18. N.J. Song, C. Lu, C.M. Chen, C. Ma, Q.Q. Kong, Z. Liu, X.X. Wei and Y.H. Li, *Mater. Des*. 109(2016)227.
19. M. Periasamy and M. Thirumalaikumar, *J. Organomet. Chem*. 609 (2000)137.
20. D. Pasero, N. Reeves and A.R. West, *J. Power Sources*, 141(2005) 156.
21. L. Wang, Y. Li, Z. Han, L. Chen, B. Qian, X. Jiang, J. Pinto and G. Yang, *J. Mater. Chem*. A 1(2013) 8385.
22. L. Xiong, Q. Long, Y. Wang, Y. Xiang, X. Wu and Z. He, *Ceram. Int*. 42(2016) 14141.
23. S. Yang, J. Miao, Q. Wang, M. Lu, J. Sun and T. Wen, *Appl. Surf. Sci*., 389 (2016):428.
24. J. Chen, X. Xia, J. Tu, Q. Xiong, Y.X. Yu, X. Wang and C. Gu*, J. Mater. Chem*., 22 (2012)15056.
25. J.G. Wang, D. Jin, R. Zhou, X. Li, X.R. Liu, C. Shen, K. Xie, B. Li, F. Kang and B. Wei, *ACS Nano*, 10 (2016) 6227.